Time-Dependent Reliability Analysis Using a Vine-ARMA Load Model

Zhen Hu
Department of Civil
and Environmental Engineering,
Vanderbilt University,
279 Jacobs Hall,
Nashville, TN 37235
e-mail: zhen.hu@vanderbilt.edu

Sankaran Mahadevan[1]
Department of Civil
and Environmental Engineering,
Vanderbilt University,
272 Jacobs Hall,
Nashville, TN 37235
e-mail: sankaran.mahadevan@vanderbilt.edu

A common strategy for the modeling of stochastic loads in time-dependent reliability analysis is to describe the loads as independent Gaussian stochastic processes. This assumption does not hold for many engineering applications. This paper proposes a Vine-autoregressive-moving average (Vine-ARMA) load model for time-dependent reliability analysis, in problems with a vector of correlated non-Gaussian stochastic loads. The marginal stochastic processes are modeled as univariate ARMA models. The correlations among different univariate ARMA models are captured using the Vine copula. The ARMA model maintains the correlation over time. The Vine copula represents not only the correlation among different ARMA models but also the tail dependence of different ARMA models. Therefore, the developed Vine-ARMA model can flexibly model a vector of high-dimensional correlated non-Gaussian stochastic processes with the consideration of tail dependence. Due to the complicated structure of the Vine-ARMA model, new challenges are introduced in time-dependent reliability analysis. In order to overcome these challenges, the Vine-ARMA model is integrated with a single-loop Kriging (SILK) surrogate modeling method. A hydrokinetic turbine blade subjected to a vector of correlated river flow loads is used to demonstrate the effectiveness of the proposed method. [DOI: 10.1115/1.4034805]

Keywords: time-dependent, reliability, time series, vine copula, stochastic process

1 Introduction

In problems with stochastic load histories and time-dependent factor, such as material degradation, wear, and corrosion, the reliability is also time-dependent [1–3]. Time-dependent reliability has been investigated intensively during the past decades using upcrossing rate methods [4–7], sampling-based methods [8–11], and surrogate modeling methods [12,13]. A common strategy in current time-dependent reliability analysis methods is to assume the stochastic loads as Gaussian stochastic processes [11] with precisely known mean, variance, and correlation functions. Based on the representation of Gaussian stochastic processes, the non-Gaussian stochastic processes are simulated based on probability transformations [14]. The most commonly used methods for the simulation of Gaussian stochastic processes include Karhunen–Loève (KL) expansion [15], orthogonal series expansion (OSE) [16], and polynomial chaos expansion [15].

Along with the above methods, ARMA modeling, which is the focus of this paper, has also been used in the time-dependent reliability analysis to describe the loading time histories based on the available experimental or history data. For instance, Singh and Mourelatos described the roughness of the road as an ARMA model for the time-dependent reliability analysis of automotive vehicles [8]; Hu et al. [17,18] used a Bayesian ARMA model to represent the stochastic load history in the time-dependent reliability analysis in the presence of parametric uncertainty; Ling et al. [19,20] described the fatigue load history as an ARMA and autoregressive-integrated moving average (ARIMA) model to perform fatigue life prognosis; and Wang and Billinton applied the ARMA model to the reliability analysis of an electric power system under the stochastic wind speed [21].

The above methods and applications of ARMA models mainly focus on a single Gaussian stochastic process or multiple independent Gaussian stochastic processes. In practical situations, however, it is quite possible that the stochastic processes are correlated and non-Gaussian. For example, the ocean waves acting on a jack-up platform are correlated at different locations of the platform [22], and the wind pressures on a building are correlated at different locations and directions [23]. A possible way of describing the high-dimensional correlated Gaussian stochastic processes is to use the multivariate ARMA models [24,25]. The basic principle of the multivariate ARMA model is to represent the noise terms as a multivariate normal distribution at each time instant [26]. The correlations of the stochastic processes over time are captured by the marginal ARMA model, and the correlations among different ARMA models are described by the multivariate normal distribution. The employment of the multivariate normal distribution in multivariate ARMA models, however, has two main limitations. First, the multivariate normal distribution is applicable only for noise terms with Gaussian marginal distribution. Second, the multivariate normal distribution cannot capture the tail dependence among different ARMA models [27]. Tail dependence refers to the phenomenon that two correlated random variables also have dependence between their extreme values. For example, there is a high probability that the rain takes its extreme value when the wind takes its extreme value during a hurricane. Accounting for the tail dependence is important in reliability analysis, because failures are usually caused by extreme events.

This paper investigates the integration of Vine copula concepts with the ARMA models to develop a Vine-ARMA model to overcome the above-mentioned limitations. Vine is a decomposition strategy, which decomposes a high-dimensional copula into bivariate copulas [28]. A reason Vine is very useful is that current multivariate copula is available only for Gaussian copula or Gaussian-related copula. When a Gaussian copula is not applicable, other copula families (such as Clayton, Gumbel, and Frank) are well studied only for bivariate cases. The decomposition using Vine enables us to flexibly model a high-dimensional copula based on currently available bivariate non-Gaussian copulas. An advantage of using the non-Gaussian bivariate copula to model the high-dimensional copula is that the tail dependence among different variables can be captured using the non-Gaussian copula. Since the first construction [29] and

[1]Corresponding author.

Manuscript received April 6, 2016; final manuscript received September 12, 2016; published online November 21, 2016. Assoc. Editor: Michael Beer.

formal definition [30] of Vines in the 1990s, they have been intensively studied in many areas [31]. Recently, Jiang et al. [27] applied Vine copula to reliability analysis by integrating Vine copula with MCS and FORM. In this work, the Vine copula is integrated with ARMA models to model high-dimensional correlated non-Gaussian load processes.

The developed Vine-ARMA model is then applied to time-dependent reliability analysis. Since current time-dependent reliability analysis methods are mainly developed based on the Gaussian and independent assumptions of stochastic loads, the introduction of the Vine-ARMA model into time-dependent reliability analysis raises new challenges. During the past years, a group of time-dependent reliability analysis methods have been developed to improve the accuracy of reliability analysis. These methods, however, cannot be directly applied to problems with Vine-ARMA models. How to accurately perform time-dependent reliability analysis is the first challenge. A surrogate modeling approach might be a promising way for problems with loads described as Vine-ARMA models. Current surrogate model-based time-dependent reliability analysis methods, however, mainly focus on problems without stochastic processes [12,13]. How to integrate the Vine-ARMA model with the surrogate model-based methods to efficiently perform time-dependent reliability analysis is the second challenge. In order to overcome these challenges, the Vine-ARMA model is combined with a recently developed SILK surrogate modeling method [32]. The combination of the Vine-ARMA model and the SILK method enables us to accurately and efficiently evaluate the time-dependent reliability. The main contributions of this paper are, therefore, summarized as: (1) the application of Vine copula in time-dependent reliability analysis, (2) the integration of Vine copula and ARMA techniques for the modeling of high-dimensional correlated non-Gaussian stochastic processes, and (3) the synthesis of Vine-ARMA and SILK for efficient and accurate time-dependent reliability analysis.

The remainder of the paper is organized as follows: Section 2 provides background review of the time-dependent reliability analysis methods and multivariate ARMA modeling. Section 3 develops a Vine-ARMA model for the modeling of high-dimensional non-Gaussian stochastic loads. Section 4 develops a method for time-dependent reliability analysis by using the Vine-ARMA model and SILK method. A turbine blade example is used to demonstrate the proposed method in Sec. 5, and concluding remarks are given in Sec. 6.

2 Background

2.1 Time-Dependent Reliability. In time-dependent reliability analysis, the first-passage reliability over a desired time period is given by [33]

$$R(t_0, t_e) = \Pr\{G(\tau) = g(\mathbf{X}, \mathbf{Y}(\tau), \tau) \le 0, \quad \forall\, \tau \in [t_0, t_e]\} \tag{1}$$

in which $G(t) = g(\mathbf{X}, \mathbf{Y}(t), t)$ is a time-dependent response function, $\mathbf{X} = [X_1, X_2, \ldots, X_n]$ is a vector of random variables, $\mathbf{Y}(t) = [Y_1(t), Y_2(t), \ldots, Y_m(t)]$ is a vector of stochastic processes, t stands for time, $\Pr\{\cdot\}$ stands for probability, "$\forall$" means "for all," and t_0 and t_e are the initial and final time instants, respectively.

The corresponding time-dependent failure probability is given by

$$p_f(t_0, t_e) = \Pr\{G(\tau) = g(\mathbf{X}, \mathbf{Y}(\tau), \tau) > 0, \quad \exists\, \tau \in [t_0, t_e]\} \tag{2}$$

where "$\exists$" means "there exists."

In practical applications, the stochastic processes $\mathbf{Y}(t) = [Y_1(t), Y_2(t), \ldots, Y_m(t)]$ may be correlated. Since the focus of this paper is to use time series models to represent stochastic processes, next, we briefly review the multivariate ARMA model which can be applied to the modeling of multiple correlated stochastic processes.

2.2 Multivariate Autoregressive-Moving Average Model. Data-driven time series models have been widely used in many areas for modeling of stochastic processes and performing predictions based on modeling. The commonly used time series models include the autoregressive (AR) model, moving average (MA) model, and ARMA model. The AR, MA, and ARMA are for stationary stochastic processes. When the stochastic process is nonstationary, the ARIMA model is employed [34]. In this work, the ARMA model is used to illustrate the proposed method. The proposed method, however, can be easily extended to ARIMA models.

An ARMA (p, q) time series model of a stochastic process $Y(t)$ is given by

$$\begin{aligned} Y(t_i) = {} & \varphi^{(0)} + \varphi^{(1)} Y(t_{i-1}) + \varphi^{(2)} Y(t_{i-2}) + \cdots + \varphi^{(p)} Y(t_{i-p}) \\ & + \varepsilon(t_i) - \omega^{(1)} \varepsilon(t_{i-1}) - \cdots - \omega^{(q)} \varepsilon(t_{i-q}) \end{aligned} \tag{3}$$

in which $\varepsilon(t_i), \varepsilon(t_{i-1}), \ldots, \varepsilon(t_{i-q})$ is a sequence of independent and identically distributed random variables with zero mean and finite standard deviation σ_ε; $\varphi^{(0)}, \varphi^{(1)}, \ldots, \varphi^{(p)}, \omega^{(1)}, \ldots, \omega^{(q)}$ are the coefficients of the ARMA model; p is the order of the AR model; and q is the order of the MA model. The random variables, $\varepsilon(t_i), \varepsilon(t_{i-1}), \ldots, \varepsilon(t_{i-q})$, can follow Gaussian or non-Gaussian distributions. The common approach is to assume that $\varepsilon(t_i), \varepsilon(t_{i-1}), \ldots, \varepsilon(t_{i-q})$ follow Gaussian distributions.

For the multivariate ARMA model, Eq. (3) is rewritten as [35]

$$\begin{aligned} Y_j(t_i) = {} & \varphi_j^{(0)} + \varphi_j^{(1)} Y_j(t_{i-1}) + \varphi_j^{(2)} Y_j(t_{i-2}) + \cdots + \varphi_j^{(p_j)} Y_j(t_{i-p_j}) \\ & + \varepsilon_j(t_i) - \omega_j^{(1)} \varepsilon_j(t_{i-1}) - \cdots - \omega_j^{(q_j)} \varepsilon_j(t_{i-q_j}), \\ & j = 1, 2, \ldots, m \end{aligned} \tag{4}$$

in which $Y_j(t_i)$ is the jth stochastic process at time instant t_i and $E(\varepsilon_j(t_i)) = 0$, $E(\varepsilon_j(t_i)\,\varepsilon_j(t_i)) = \sigma_{\varepsilon_j}^2$, $E(\varepsilon_j(t_i)\varepsilon_k(t_i)) = \rho_{j_k}\sigma_{\varepsilon_j}\sigma_{\varepsilon_k}$, and $E(\varepsilon_j(t_i)\varepsilon_k(t_l)) = 0$, $\forall i \neq l$, where ρ_{jk} is the correlation coefficient between noise terms $\varepsilon_j(t_i)$ and $\varepsilon_k(t_i)$ at time instant t_i.

In practical situations, we may know only (if at all) the correlation between $Y_i(t)$ and $Y_j(t)$, $\forall i, j = 1, 2, \ldots, m$. The correlation between the noise terms of the multivariate ARMA models is then obtained by solving the following equation [35]:

$$\Sigma_Y = \boldsymbol{\varphi} \Sigma_Y \boldsymbol{\varphi}^T + \boldsymbol{\omega} \Sigma_\varepsilon \boldsymbol{\omega}^T \tag{5}$$

where Σ_Y is the covariance matrix of $Y_i(t)$ and $Y_j(t)$, $\forall i, j = 1, 2, \ldots, m$; Σ_ε is the covariance matrix of $\varepsilon_i(t)$ and $\varepsilon_j(t)$, $\forall i, j = 1, 2, \ldots, m$; and $\boldsymbol{\varphi}$ and $\boldsymbol{\omega}$ are the coefficients matrices with the ith row being the coefficients of the ith ARMA model (i.e., $[\varphi_i^{(1)}, \varphi_i^{(2)}, \ldots, \varphi_i^{(p)}]$ and $[\omega_i^{(1)}, \omega_i^{(2)}, \ldots, \omega_i^{(q)}]$).

Based on the multivariate ARMA model, the non-Gaussian stochastic processes are then obtained using the probability transformation as follows:

$$Z(t) = F_Z^{-1}(\Phi(Y(t), \mu_Y, \sigma_Y)) \tag{6}$$

in which $F_Z(\cdot)$ is the marginal cumulative probability function (CDF) of a non-Gaussian stochastic process $Z(t)$; $F_Z^{-1}(\cdot)$ is the inverse CDF; μ_Y and σ_Y are the mean and standard deviation of Gaussian stochastic process $Y(t)$; and $\Phi(\cdot, \mu, \sigma)$ is the CDF of a normal variable.

Even though multivariate ARMA models can effectively model and simulate the correlated stochastic processes, their application is limited by two main drawbacks: (1) the marginal distribution of the noise term is limited to Gaussian distribution since the Gaussian distribution can significantly facilitate the regression of ARMA models and (2) the multivariate Gaussian distribution cannot capture the tail dependence between different load processes. In Sec. 3, the Vine copula is integrated with ARMA models to overcome the drawbacks of multivariate ARMA models.

3 Vine-ARMA Model for High-Dimensional Stochastic Load Modeling

This section first introduces the concepts of tail dependence and Vine copula, followed by development of the proposed Vine-ARMA model.

3.1 Tail Dependence. Tail dependence, which is usually defined for bivariate random variables, measures the extreme comovements in the lower and upper tails of the joint probability function [36]. In other words, tail dependence gives the probability that a random variable reaches an extreme value given that another random variable attains an extreme value as well. For two random variables X_1 and X_2, the upper tail dependence coefficient (UTDC) λ_U and the lower tail dependence coefficient (LTDC) λ_L are defined as [36]

$$\lambda_U = \lim_{u \to 1^-} \Pr\{X_2 > F_2^{-1}(u) | X_1 > F_1^{-1}(u)\} \tag{7}$$

$$\lambda_L = \lim_{u \to 0^+} \Pr\{X_2 \le F_2^{-1}(u) | X_1 \le F_1^{-1}(u)\} \tag{8}$$

where u is the CDF value of a random variable, $u \to 0^+$ means u approaches 0 from the value larger than 0 side, $u \to 1^-$ means u approaches 1 from the value less than 1 side, and $F_1^{-1}(\cdot)$ and $F_2^{-1}(\cdot)$ are the inverse CDFs of X_1 and X_2, respectively.

The UTDC and LTDC can also be represented in terms of copula functions [36]. A copula function describes the dependence between random variables by linking the marginal probability functions to the joint distribution function [37]. For n random variables, $X_1, X_2, \ldots, X_n$, the joint CDF $F(x_1, x_2, \ldots, x_n)$ is connected to the marginal CDFs using the copula function C as follows:

$$\begin{aligned} F(x_1, x_2, \ldots, x_n) &= C(F_1(x_1), F_2(x_2), \ldots, F_n(x_n)) \\ &= C(F_1^{-1}(u_1), F_2^{-1}(u_2), \ldots, F_n^{-1}(u_n)) \end{aligned} \tag{9}$$

where $F_i(\cdot)$ is the CDF of the ith random variable; $F_i^{-1}(\cdot)$ is the corresponding inverse CDF; and u_i is the marginal CDF value of x_i.

Using the copula function, UTDC and LTDC are represented as [36]

$$\lambda_U = \lim_{u \to 1^-} \frac{1 - 2u + C(u, u)}{1 - u} \tag{10}$$

$$\lambda_L = \lim_{u \to 0^+} \frac{C(u, u)}{u} \tag{11}$$

It has been shown that both UTDC and LTDC are zero for the bivariate normal distribution [36]. Since the multivariate normal distribution can be represented as combinations of bivariate normal distributions or a multivariate Gaussian copula, this means that the tail dependence between individual ARMA models cannot be captured in the multivariate ARMA models presented in Sec. 2.2. Tail dependence is important for both time-independent and time-dependent reliability analyses, as failure events are often caused by extreme (rare) events. The non-Gaussian copulas are able to capture the tail dependence between two random variables. But current non-Gaussian copulas are well studied only for bivariate distributions. In order to represent the correlations over time and between individual ARMA models and at the same time capture their tail dependences, a promising way is to integrate Vine copula with ARMA models. Note that Levy process has also been used to capture the anomalous tail behaviors and correlation structure of a stochastic process [38,39]. However, the focus of this paper is to capture the tail dependence between different stochastic processes. The Vine-ARMA model presented in this paper can be extended to capture the tail dependence between different Levy processes by developing a Vine-Levy model.

3.2 Vine Copula. During the past decades, numerous methods have been developed to model the extreme value distributions and perform load combination of extreme value distributions [40–42]. Most of these methods, however, are based on certain assumptions and simplifications. In this paper, the Vine copula is employed to develop a more rigorous way of modeling the extreme values of loads. As discussed in the above sections, using a multivariate Gaussian distribution cannot capture the tail dependence between load processes. In this situation, the high-dimensional copula can facilitate the correlation representation and tail dependence modeling of high-dimensional variables, as the marginal distribution of the correlated random variables is independent of the copula function. However, most of the copula families, which can capture the tail dependence, are well studied only for bivariate cases.

Vine is a method used to represent a high-dimensional probability distribution of correlated random variables through bivariate copulas. Based on the bivariate decomposition, we can then use the well-studied non-Gaussian bivariate copulas to model the complicated dependences among multiple random variables [28]. The basic principle of Vine decomposition is that the joint probability density function (PDF) of n random variables, $X_1, X_2, \ldots, X_n$, can be decomposed as

$$\begin{aligned} f(x_1, x_2, \ldots, x_n) &= f_n(x_n) \cdot f(x_{n-1}|x_n) \\ &\quad \cdot f(x_{n-2}|x_{n-1}, x_n) \cdots f(x_1|x_2, \ldots, x_n) \end{aligned} \tag{12}$$

where $f(\cdot \mid \cdot)$ is the conditional PDF.

There are many possible combinations of the decomposition. The above decomposition is used as an example just to illustrate the principle of Vine. For any conditional PDF, $f(x|\mathbf{x}^C)$, it can be represented as pair-copula density functions as follows [43]:

$$f(x|\mathbf{x}^C) = c_{xc_j|\mathbf{c}-}\{F(x|\mathbf{x}^{C-}), F(x_j^C|\mathbf{x}^{C-})\} f(x|\mathbf{x}^{C-}) \tag{13}$$

where x_j^C is an arbitrarily chosen variable among the conditioned variables $\mathbf{x}^C$; $\mathbf{x}^{C-}$ is the set of conditioned variables excluding the chosen variable x_j^C; $c_{xc_j|\mathbf{c}-}\{\cdot,\cdot\}$ is the bivariate copula density function; and $F(x|\mathbf{x}^{C-})$ is the conditional CDF [43].

As indicated in Eq. (13), a key step in the Vine decomposition is the computation of the conditional CDF $F(x|\mathbf{x}^{C-})$. For a generalized $F(x_1|x_2)$, it has been shown that [44]

$$F(x_1|x_2) = h(u, v, \Theta) = \frac{\partial C_{12}\{F_1(x_1), F_2(x_2)\}}{\partial F_2(x_2)} = \frac{\partial C_{12}\{u, v\}}{\partial v} \tag{14}$$

where $C_{12}\{\cdot,\cdot\}$ is the bivariate copula function; Θ is the vector of parameters of the copula; $u = F_1(x_1)$; and $v = F_2(x_2)$. When the conditioning variables are multivariate, similar expressions can be found in Ref. [43]. The h-function given in Eq. (14) has been derived for commonly used bivariate Gaussian, Student's t test, Clayton, and Gumbel copulas in Ref. [43]. Based on the h-functions, the conditional PDF given in Eq. (13) can be computed.

It should be noted that there are many possible Vines to describe the joint PDF given in Eq. (12), as the joint PDF can be decomposed in different orders. For example, $f(x_1|x_2, x_3)$ can be decomposed as

$$f(x_1|x_2, x_3) = c_{12|3}\{F(x_1|x_3), F(x_2|x_3)\} \cdot f(x_1|x_3) \tag{15}$$

or

$$f(x_1|x_2, x_3) = c_{13|2}\{F(x_1|x_2), F(x_3|x_2)\} \cdot f(x_1|x_2) \tag{16}$$

Even if there are many possible Vines, not all Vines can be used to obtain a pair copula construction, and the most commonly used Vines include the D-Vine and C-Vine. A vine structure that is consistent with a valid pair copula construction is called the regular Vine [45]. D-Vine and C-Vine are special cases of the regular Vine. There are also other regular Vines that can represent Eq. (12)

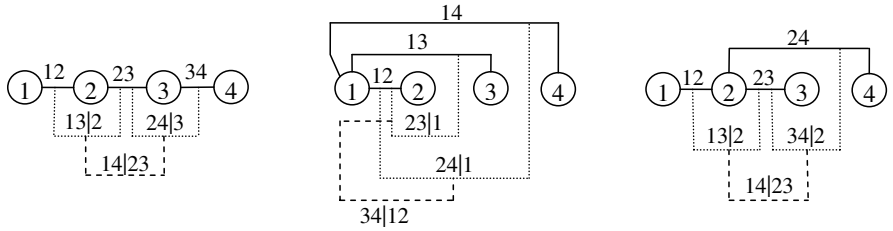

Fig. 1 Four-variable (node) Vine models: (*a*) D-Vine, (*b*) C-Vine, and (*c*) a regular Vine

flexibly. The joint PDF given in Eq. (12) is decomposed using a D-Vine as [43,46,47]

$$f(x_1, x_2, \ldots, x_n) = \prod_{i=1}^{n} f_i(x_i) \prod_{j=1}^{n-1} \prod_{i=1}^{n-j} c_{i,i+j|i+1,\ldots,i+j-1} \times \{F(x_i|x_{i+1}, \ldots, x_{i+j-1}), \times F(x_{i+j}|x_{i+1}, \ldots, x_{i+j-1})\} \tag{17}$$

The C-Vine decomposition gives [43,46,47]

$$f(x_1, x_2, \ldots, x_n) = \prod_{i=1}^{n} f_i(x_i) \prod_{j=1}^{n-1} \prod_{i=1}^{n-j} c_{j,j+i|1,\ldots,j-1} \times \{F(x_j|x_1, \ldots, x_{j-1}), F(x_{j+i}|x_1, \ldots, x_{j-1})\} \tag{18}$$

We use a four-variable problem below to illustrate the differences among different Vines. Figure 1 shows the D-Vine, C-Vine, and a regular Vine decomposition of the joint PDF of four random variables.

The previous discussion indicates that a high-dimensional joint distribution can be decomposed into bivariate copulas using Vines. This enables us to use non-Gaussian bivariate copulas to model complicated high-dimensional dependences instead of using multivariate Gaussian distributions. Next, we will develop the proposed integration of Vine and ARMA models.

3.3 Vine-ARMA Model for Correlated Load Process Modeling. The basic principle for the integration of Vine copula with ARMA models is to implement a *top-down* procedure during the simulation process of the multivariate ARMA model. It is different from the conventional multivariate ARMA models that implement a *bottom-up* procedure. More specifically, during the conventional simulation of multivariate ARMA models, realizations of the noise terms, $\varepsilon_j(t)$, $j = 1, 2, \ldots, m$, are generated first. Based on realizations of the noise terms, realizations of the stochastic processes are obtained. However, in the proposed Vine-ARMA model, samples are generated at the stochastic process response level (physical quantity level) first. The generated samples are then transformed to the noise terms to simulate the ARMA models.

The top-down procedure for the integration of Vine and ARMA is achieved through the distribution-independent property of the copula function. For m non-Gaussian stochastic processes $Z_1(t), Z_2(t), \ldots, Z_m(t)$, at a specific time instant t, we have

$$F(z_1(t), z_2(t), \ldots, z_m(t)) = C(F_{Z_1}(z_1(t)), F_{Z_2}(z_2(t)), \ldots, F_{Z_m}(z_m(t))) \tag{19}$$

in which $F_{Z_i}(\cdot)$ is the CDF of the ith stochastic process.

According to the probability transformation given in Eq. (6), Eq. (19) can be rewritten in terms of the associated ARMA models $Y_1(t), Y_2(t), \ldots, Y_m(t)$ as

$$F(z_1(t), z_2(t), \ldots, z_m(t)) = C(u_1, u_2, \ldots, u_m) = C(\Phi(y_1(t), \mu_{Y_1}, \sigma_{Y_1}), \Phi(y_2(t), \mu_{Y_2}, \sigma_{Y_2}), \ldots, \Phi(y_m(t), \mu_{Y_m}, \sigma_{Y_m})) \tag{20}$$

where $y_j(t)$ is a realization of the stochastic process $Y_j(t)$ at time instant t, $j = 1, 2, \ldots, m$.

For any ARMA model $Y_j(t)$, the realization at time instant t_i is a random variable conditioned on realizations before this time instant and is given by

$$Y_j(t_i) = \varphi_j^{(0)} + \varphi_j^{(1)} y_j(t_{i-1}) + \varphi_j^{(2)} y_j(t_{i-2}) + \cdots + \varphi_j^{(p)} y_j(t_{i-p}) + \varepsilon_j(t_i) - \omega_j^{(1)} \varepsilon_j(t_{i-1}) - \cdots - \omega_j^{(q)} \varepsilon_j(t_{i-q}) \tag{21}$$

Equation (21) can be rewritten as

$$Y_j(t_i)|y_j(t_{i-1}), \ldots, y_j(t_{i-1}), \varepsilon_j(t_{i-1}), \ldots, \varepsilon_j(t_{i-q}) = a_j + \varepsilon_j(t_i) \tag{22}$$

where

$$a_j = \varphi_j^{(0)} + \varphi_j^{(1)} y_j(t_{i-1}) + \varphi_j^{(2)} y_j(t_{i-2}) + \cdots + \varphi_j^{(p)} y_j(t_{i-p}) - \omega_j^{(1)} \varepsilon_j(t_{i-1}) - \cdots - \omega_j^{(q)} \varepsilon_j(t_{i-q}) \tag{23}$$

The above equation implies that $Y_j(t_i)|y_j(t_{i-1}), \ldots, y_j(t_{i-1}), \varepsilon_j(t_{i-1}), \ldots, \varepsilon_j(t_{i-q})$ is a linear function of $\varepsilon_j(t_i)$, and we have

$$F_Y(Y_j(t_i)|y_j(t_{i-1}), \ldots, y_j(t_{i-1}), \varepsilon_j(t_{i-1}), \ldots, \varepsilon_j(t_{i-q}) < y^*) = F_\varepsilon(\varepsilon(t_i) < (y^* - a_j)) \tag{24}$$

Based on Eqs. (20) and (24), we then have

$$F(z_1(t), z_2(t), \ldots, z_m(t)) = C(u_1, u_2, \ldots, u_m) = C(F_{\varepsilon_1}(\varepsilon_1(t)), F_{\varepsilon_2}(\varepsilon_2(t)), \ldots, F_{\varepsilon_m}(\varepsilon_m(t))) \tag{25}$$

Equation (25) indicates that the copula at the stochastic process response level (physical quantity level) is the same as the copula at the noise-term level in the conventional ARMA models. This property significantly facilitates the integration of the Vine and ARMA models.

In order to use the Vine copula to capture the tail dependence among different ARMA models, we build a Vine copula model to capture the dependence at any given time instant and use the univariate ARMA models to maintain the correlation over time. The Vine copula and the univariate ARMA model are connected through the CDF values in the copula function as indicated in Eq. (25). Next, we will first briefly discuss how to build such a Vine-ARMA model based on data. Following that, we will explain the simulation of the Vine-ARMA model.

3.4 Construction of the Vine-ARMA Model. Since the Vine copula is a function of CDF values and is independent from the marginal distribution types of the univariate ARMA models and the noise terms, the Vine copula and the univariate ARMA models can be built independently.

During the construction of the Vine-ARMA model, the experimental data on $Z_1(t), Z_2(t), \ldots, Z_m(t)$ are first transformed into data on CDF values and data on the associated standard Gaussian stochastic processes based on the marginal distributions of the stochastic processes. The data on the CDF values are then used to build the Vine copula, and the data on the associated Gaussian stochastic processes are used to build the individual ARMA models. The construction of the Vine copula involves the selection of Vine structure and copula types. Once the Vine structure and copula type are determined, parameters of the bivariate copulas need to be estimated. The construction of the Vine copula has been well studied in the literature and is not the focus of this paper; we direct the readers to Refs. [43,46,47] for details. The methods for the construction of univariate ARMA models are also well-documented, such as the Yule-Walker method, Burg method, covariance method, and maximum likelihood estimation [34,48]. In this work, we, therefore, do not give details about how to construct the ARMA models. Note that the Vine tree structure, the copula type, and copula parameters may affect the reliability analysis results. As mentioned above, the selection of Vine copula has been studied in Refs. [43,46,47,49] using either maximum likelihood-based method or Bayesian methods. More details about the selection of Vine copula can be found in Refs. [43,46,47,49]. The Vine-ARMA model and the associated reliability analysis method developed in the subsequent sections are based on the assumption that the Vine copula is already selected based on available data.

Assume that from the construction, we obtain the parameters of the bivariate copula function as $\Theta_{j,i}$ (the parameters given in Eqs. (17) and (18)) and the parameters of the univaraite ARMA models as $\boldsymbol{\varphi}$ and $\boldsymbol{\omega}$ (the coefficients given in Eq. (5)). Next, we will discuss how to simulate the Vine-ARMA model based on $\Theta_{j,i}$, $\boldsymbol{\varphi}$, and $\boldsymbol{\omega}$.

3.5 Simulation of Vine-ARMA Model. At a given time instant t, there are two widely used methods that can be employed for the simulation of correlated random variables: the Rosenblatt transformation [50] and the Nataf transformation [51]. The Nataf transformation is basically the multivariate Gaussian copula, which cannot capture the tail dependence. The Rosenblatt transformation is accurate but requires the joint CDF of the correlated random variables. Since the joint CDF and tail dependence of the high-dimensional load processes are accurately described by the Vine copula, the Rosenblatt transformation can be used to simulate the load processes at the given time instant.

As discussed in Secs. 3.1 to 3.3, the simulation of the Vine-ARMA model is implemented here through a *top-down* procedure. For a given time instant t, we first generate samples of the physical quantity $Z_1(t), Z_2(t), \ldots, Z_m(t)$. Since $Z_1(t), Z_2(t), \ldots, Z_m(t)$ are high-dimensional correlated random variables at a given time instant, the Rosenblatt transformation [50] generates samples for $Z_1(t), Z_2(t), \ldots, Z_m(t)$ as follows:

$$\begin{aligned} u_1^{in} &= F_{Z_1}(z_1(t)) \\ u_2^{in} &= F_{Z_2|Z_1}(z_2(t)|z_1(t)) \\ u_3^{in} &= F_{Z_3|Z_2,Z_1}(z_3(t)|z_2(t), z_1(t)) \\ &\vdots \\ u_m^{in} &= F_{Z_m|Z_{m-1},\ldots,Z_2,Z_1}(z_m(t)|z_{m-1}(t), \ldots, z_2(t), z_1(t)) \end{aligned} \tag{26}$$

where $u_1^{in}, u_2^{in}, \ldots, u_m^{in}$ are samples generated from independent uniform random variables $[0, 1]$.

Since the samples of $Z_1(t), Z_2(t), \ldots, Z_m(t)$ are connected to the noise term through the copula equivalence given in Eq. (25), Eq. (26) can be rewritten in terms of copula functions as

$$\begin{aligned} u_1^{in} &= u_1^{Co} \\ u_2^{in} &= \frac{\partial C_{12}(F(z_2(t)), F(z_1(t)))}{\partial F(z_1(t))} = h(u_2^{Co}, u_1^{Co}, \Theta_{11}) \\ u_3^{in} &= \frac{\partial C_{32|1}(F(z_3(t)|z_1(t)), F(z_2(t)z_1(t)))}{\partial F(z_2(t)|z_1(t))} \\ &= h(h(u_3^{Co}, u_1^{Co}, \Theta_{12}), h(u_2^{Co}, u_1^{Co}, \Theta_{11}), \Theta_{21}) \\ &\vdots \end{aligned} \tag{27}$$

Based on Eq. (27), correlated CDF samples of $Z_1(t), Z_2(t), \ldots, Z_m(t)$ are obtained as below

$$\begin{aligned} u_1^{Co} &= u_1^{in} \\ u_2^{Co} &= h^{-1}(u_2^{in}, u_1^{Co}, \Theta_{11}) \\ u_3^{Co} &= h^{-1}(h^{-1}(u_3^{in}, h(u_2^{Co}, u_1^{Co}, \Theta_{11}), \Theta_{21}), u_1^{Co}, \Theta_{12}) \\ &\vdots \end{aligned} \tag{28}$$

in which $u_1^{Co}, u_2^{Co}, \ldots, u_m^{Co}$ are correlated CDF samples of $Z_1(t), Z_2(t), \ldots, Z_m(t)$ or of $\varepsilon_1(t), \varepsilon_2(t), \ldots, \varepsilon_m(t)$ at time instant t.

Note that the inverse h-function (i.e., $h^{-1}(\cdot, \cdot, \Theta)$) is required to generate the CDF samples. The inverse h-function for commonly used Gaussian, Clayton, Student's t, and Gumbel copulas can be found in Ref. [43]. For different Vine structures, the sampling orders of the CDF values are different. Typically, the C-Vine is computationally more efficient than the D-Vine, as the C-Vine has fewer numbers of conditional distribution functions to be computed in the simulation than the D-Vine. In this work, the C-Vine is used in the Vine-ARMA model.

Once the samples of $u_1^{Co}, u_2^{Co}, \ldots, u_m^{Co}$ are obtained, samples of $\varepsilon_1(t), \varepsilon_2(t), \ldots, \varepsilon_m(t)$ are obtained as

$$\varepsilon_i(t) = F_{\varepsilon_i}^{-1}(u_i^{Co}) \tag{29}$$

where $F_{\varepsilon_i}^{-1}(\cdot)$ is the inverse CDF of $\varepsilon_i(t)$.

Based on the samples of $\varepsilon_1(t), \varepsilon_2(t), \ldots, \varepsilon_m(t)$, samples of $Y_1(t), Y_2(t), \ldots, Y_m(t)$ and $Z_1(t), Z_2(t), \ldots, Z_m(t)$ at time instant t conditioned on realizations before this time instant are then obtained using Eqs. (21)–(23) and the coefficients of the ARMA models. Table 1 gives a simplified algorithm for the simulation of the Vine-ARMA model based on the C-Vine structure. In the algorithm, the simulation algorithm of the Vine structure is adopted from Ref. [43]. The discussions presented in Secs. 3.3–3.5 show that no Gaussian assumption is made regarding the noise term of the ARMA models. Therefore, the developed Vine-ARMA model is also applicable to multivariate ARMA models with non-Gaussian noise terms. This advantage comes from the distribution-type independence property of the copula function.

Table 1 Algorithm to generate a realization of the Vine-ARMA model

For it=1 to n_t, where n_t is the number of time instants to be simulated

  Generate samples $u_1^{in}, u_2^{in}, \cdots, u_m^{in}$ from independent uniform distribution $[0,1]$

  $u_1^{Co} = u_{temp}(1,1) = u_1^{in}$

  For i=2 to n

    $u_{temp}(i,1) = u_i^{in}$

    For k=i-1 to 1

      $u_{temp}(i,1) = h^{-1}(u_{temp}(i,1), u_{temp}(k,k), \Theta_{k,i-k})$

    End

    $u_i^{Co} = u_{temp}(i,1)$

    If i==n

      Stop

    End if

    For j=1 to i-1

      $u_{temp}(i, j+1) = h(u_{temp}(i, j), u_{temp}(j, j), \Theta_{j,i-j})$

    End

  End

  Convert $u_1^{Co}, u_2^{Co}, \cdots, u_m^{Co}$ into $\varepsilon_1(t_{it}), \varepsilon_2(t_{it}), \cdots, \varepsilon_m(t_{it})$ using Eq. (29).

  Obtain samples of $y_1(t_{it}), y_2(t_{it}), \cdots, y_m(t_{it})$ using Eqs. (21)-(23).

  Obtain $z_1(t_{it}), z_2(t_{it}), \cdots, z_m(t_{it})$ using Eq. (6).

End

Next, we will develop our proposed approach to apply the Vine-ARMA model to time-dependent reliability analysis.

4 Time-Dependent Reliability Analysis Using the Vine-ARMA Model

The Vine-ARMA model is able to flexibly capture the tail dependence and correlations among different stochastic processes and over time. The complicated Vine copula structure, however, creates new challenges for time-dependent reliability analysis when the Vine-ARMA model is substituted in Eq. (2). In order to overcome the difficulty introduced by the Vine-ARMA model, a SILK surrogate modeling method recently developed by the authors is employed to perform time-dependent reliability analysis [32]. In this section, we first briefly review the SILK method. Based on that, we discuss time-dependent reliability analysis based on the combination of the SILK and Vine-ARMA models.

4.1 SILK Method for Time-Dependent Reliability Analysis. During the past decades, a group of time-dependent reliability analysis methods have been developed, such as the upcrossing rate method [6,52], composite limit-state function method [53], and extreme value surrogate modeling-based methods [12,13]. Even though the upcrossing rate methods can perform time-dependent reliability analysis for problems with stochastic processes, currently available methods cannot be applied to problems with Vine-ARMA models considering that the complicated Vine copula structure brings significant challenges to the correlation computation of the system response. The surrogate modeling-based method is a potential solution to this. Current extreme value surrogate modeling-based methods, however, have low computational efficiency for problems with stochastic processes. Recently, a SILK surrogate modeling method has been developed by the authors for the reliability analysis of problems with stochastic processes by converting the double-loop procedure in the extreme value surrogate modeling methods into a single-loop procedure. The SILK method has been found to significantly improve the efficiency of time-dependent reliability analysis without sacrificing the accuracy. In this paper, we therefore combine SILK with the Vine-ARMA model to overcome the challenges created by introducing the Vine-ARMA model. A very brief summary of the SILK method is provided here; refer to [32] for details.

The basic idea of the SILK method for time-dependent reliability analysis is to build a single surrogate model $\hat{G} = \hat{g}(\mathbf{X}, \mathbf{Y}, t)$ using the Kriging approach summarized in the Appendix. The surrogate model is refined adaptively based on a learning function, and the quality of the surrogate model is checked during the refinement using a convergence criterion. Before the training of the surrogate model $\hat{G} = \hat{g}(\mathbf{X}, \mathbf{Y}, t)$, the time interval $[t_0, t_e]$ is first discretized into N_t time instants, and N_{MCS} samples for $\mathbf{X}$ and N_{MCS} trajectories for $\mathbf{Y}(t)$ are generated. Let the prediction of the surrogate model at a sample point $[\mathbf{x}^{(i)}, \mathbf{y}^{(i)}(t^{(j)}), t^{(j)}]$ be $\hat{G}(\mathbf{x}^{(i)}, \mathbf{y}^{(i)}(t^{(j)}), t^{(j)})$. According to the property of the Kriging surrogate model, we then have

$$\hat{G}(\mathbf{x}^{(i)}, \mathbf{y}^{(i)}(t^{(j)}), t^{(j)}) \sim N(\bar{g}(\mathbf{x}^{(i)}, \mathbf{y}^{(i)}(t^{(j)}), t^{(j)}), \sigma_{\hat{g}}^2(\mathbf{x}^{(i)}, \mathbf{y}^{(i)}(t^{(j)}), t^{(j)})) \quad (30)$$

where $\bar{g}(\mathbf{x}^{(i)}, \mathbf{y}^{(i)}(t^{(j)}), t^{(j)})$ and $\sigma_{\hat{g}}^2(\mathbf{x}^{(i)}, \mathbf{y}^{(i)}(t^{(j)}), t^{(j)})$ are obtained from Eqs. (A3) and (A5), and $\mathbf{y}^{(i)}(t^{(j)})$ is the ith trajectory at time instant $t^{(j)}$.

The quality of the Kriging surrogate model is then checked using the following convergence criterion:

$$\varepsilon_r^{\max} = \max_{[N_{f2}^* \in [0, N_2]} \left\{ \frac{|N_{f2} - N_{f2}^*|}{N_{f1} + N_{f2}^*} \times 100\% \right\} \quad (31)$$

where $N_{f1} = \sum_{i=1}^{N_{\text{MCS}}} I_1(i)$ and $N_{f2} = \sum_{i=1}^{N_{\text{MCS}}} I_2(i)$, and

$$I_1(i) = \begin{cases} 1, & \text{if } \max\limits_{t\in[t_0,t_e]}\{\bar{g}(\mathbf{x}^{(i)},\mathbf{y}^{(i)}(t),t)\} > 0 \text{ and } U_{\min}(i) < 2 \\ 0, & \text{otherwise} \end{cases}, \quad \forall\ i = 1,2,\ldots,N_{\text{MCS}} \tag{32}$$

$$I_2(i) = \begin{cases} 1, & \text{if } \max\limits_{t\in[t_0,t_e]}\{\bar{g}(\mathbf{x}^{(i)},\mathbf{y}^{(i)}(t),t)\} > 0 \text{ and } U_{\min}(i) \geq 2 \\ 0, & \text{otherwise} \end{cases}, \quad \forall\ i = 1,2,\ldots,N_{\text{MCS}} \tag{33}$$

in which

$$U_{\min}(i) = \begin{cases} u_e, & \text{if } \hat{g}(\mathbf{x}^{(i)},\mathbf{y}^{(i)}(t^{(j)}),t^{(j)}) > 0 \text{ and } U(\mathbf{x}^{(i)},\mathbf{y}^{(i)}(t^{(j)}),t^{(j)}) \geq 2, \exists\, j = 1,2,\ldots,N_t \\ \min\limits_{j=1,2,\ldots,N_t}\{U(\mathbf{x}^{(i)},\mathbf{y}^{(i)}(t^{(j)}),t^{(j)})\}, & \text{otherwise} \end{cases} \tag{34}$$

where u_e is an arbitrary constant larger than two and $U(\mathbf{x}^{(i)},\mathbf{y}^{(i)}(t^{(j)}),t^{(j)})$ is given by [32,54,55]

$$U(\mathbf{x}^{(i)},\mathbf{y}^{(i)}(t^{(j)}),t^{(j)}) = \frac{|\bar{g}(\mathbf{x}^{(i)},\mathbf{y}^{(i)}(t^{(j)}),t^{(j)})|}{\sigma_{\hat{g}}(\mathbf{x}^{(i)},\mathbf{y}^{(i)}(t^{(j)}),t^{(j)})} \tag{35}$$

If $\varepsilon_r^{\max} < 5$, it means that the accuracy of surrogate model $\hat{G} = \hat{g}(\mathbf{X},\mathbf{Y},t)$ can satisfy the 5% error requirement. If the accuracy requirement is satisfied, the time-dependent failure probability is then estimated by [32]

$$p_f(t_0,t_e) = \sum_{i=1}^{N_{\text{MCS}}} I_f\Big(\max_{t\in[t_0,t_e]}\{\bar{g}(\mathbf{x}^{(i)},\mathbf{y}^{(i)}(t),t)\}\Big) \tag{36}$$

where

$$I_f\Big(\max_{t\in[t_0,t_e]}\{\bar{g}(\mathbf{x}^{(i)},\mathbf{y}^{(i)}(t),t)\}\Big) = \begin{cases} 1, & \text{if } \max\limits_{t\in[t_0,t_e]}\{\bar{g}(\mathbf{x}^{(i)},\mathbf{y}^{(i)}(t),t)\} > 0 \\ 0, & \text{otherwise} \end{cases} \tag{37}$$

If the convergence criterion is not satisfied, then a new training point is identified by

$$\mathbf{x}_{\text{new}}^t = [\mathbf{x}^{(i_{\text{new}})},\mathbf{y}^{(i_{\text{new}})}(t^{(i_{\text{new}}^t)}),t^{(i_{\text{new}}^t)}] \tag{38}$$

where

$$i_{\text{new}} = \underset{i=1,2,\ldots,N_{\text{MCS}}}{\arg\min}\ \{U_{\min}(i)\} \tag{39}$$

$$i_{\text{new}}^t = \underset{i=1,2,\ldots,N_t}{\arg\min}\ \{U(\mathbf{x}^{(i_{\text{new}})},\mathbf{y}^{(i_{\text{new}})}(t^{(i)}),t^{(i)})\} \tag{40}$$

In order to avoid the clustering of training points, another criterion is also introduced in SILK as follows [32]:

$$\max\{\boldsymbol{\rho}(\mathbf{x}_{\text{new}}^t,\mathbf{x}^s)\} < 0.95 \tag{41}$$

where $\mathbf{x}^s$ is a matrix of current training points and $\boldsymbol{\rho}(\mathbf{x}_{\text{new}}^t,\mathbf{x}^s)$ are the correlations between the new training points and current training points. The SILK method is applicable to general time-dependent reliability analysis problems with Gaussian, non-Gaussian, correlated, or independent stochastic load processes. The Vine-ARMA model, therefore, can be easily combined with SILK for time-dependent reliability analysis.

4.2 Time-Dependent Reliability Analysis Based on SILK and Vine-ARMA. We now summarize the general procedure for time-dependent reliability analysis using the SILK method and Vine-ARMA models. The Vine-ARMA model is used to accurately generate samples for the stochastic process, and SILK is used to identify training points from the generated samples to efficiently perform time-dependent reliability analysis. The Vine-ARMA model guarantees the accuracy of extreme value modeling of stochastic load and SILK reduces the computational effort of reliability analysis. Table 2 gives the generalized algorithm for time-dependent reliability analysis using the SILK and Vine-ARMA models.

Overall, the proposed method consists of mainly two parts. The Vine-ARMA model accurately captures the tail dependence between high-dimensional correlated stochastic loads, which ensures the accuracy of time-dependent reliability analysis. The combination of Vine-ARMA model and SILK method makes the time-dependent reliability analysis with Vine-ARMA models possible and efficient. The developed method is able to perform time-dependent reliability analysis accurately and efficiently. In Table 2, 5% is used as the error requirement for the surrogate modeling; this is only for the sake of illustration. The actual value is chosen by the decision-maker based on the risk tolerance for the particular problem. However, when the number is decreased (i.e., higher requirement of accuracy), the reliability estimate will become accurate but the number of training points for the surrogate model will increase. In the Section 5, we use a numerical example with a hydrokinetic turbine blade to illustrate the proposed Vine-ARMA model and the SILK-Vine-ARMA approach for time-dependent reliability analysis.

5 Numerical Example: A Hydrokinetic Turbine Blade

5.1 Problem Statement. A hydrokinetic turbine as shown in Fig. 2 is a mechanism to extract energy from river water flow [6,56]. During its operation, the turbine is subjected to stochastic flow loads. At different locations (stations) of the turbine blade, the stochastic river loads are different and correlated. In this section, the time-dependent reliability analysis of a hydrokinetic turbine blade is used to illustrate the proposed Vine-ARMA load model and the combination of SILK and Vine-ARMA methods. This example is modified from Ref. [57].

A three-dimensional model of the hydrokinetic turbine blade is shown in Fig. 3. The hydrokinetic turbine blade is 1 m long and made of steel. The turbine blade is twisted and has variable chord length along the radial direction. The hydrofoil of the turbine blade is NREL S809. The lift and drag coefficients of the hydrofoil are available in Ref. [58]. Figures 4 and 5 show the chord length and twist angle distribution of the turbine blade along the radial direction. Failure of the turbine blade is defined to occur when the maximum stress on the turbine blade is larger than the strength of the material. Note that rotation of the turbine blade is an important issue for the safety of the hydrokinetic turbine blade, because rotation will change the load conditions of the turbine system. There are also uncertainty sources in the rotation model of the blade. Considering rotation and fluid-structure interactions of the turbine system will make the problem more practical and complicated. Since the turbine blade is just an illustrative example to show the effectiveness of the

Table 2 Algorithm for time-dependent reliability analysis based on SILK and Vine-ARMA

Description

Discretize time interval $[t_0, t_e]$ into N_t time instants.

Generate initial training points and evaluate the response at the training points.

Set $q = 1$ and $\mathbf{x}^{MCS} = \varnothing$

While $q = 1$ or $Cov_{pf} > 0.05$ **do**

  Set $p = 1$

    Generate N_{MCS} trajectories of the correlated stochastic processes using the algorithm presented in **Table 1** and generate N_{MCS} samples for random variables $\mathbf{X}$. Add the generated samples into $\mathbf{x}^{MCS}$.

    While $p = 1$ or $\varepsilon_r^{\max} > 5\%$ **do**

      $p = p + 1$

      Construct surrogate model $\hat{g}(\mathbf{X}, \mathbf{Y}, t)$

      Identify new training point $[\mathbf{x}^{(i_{new})}, \mathbf{y}^{(i_{new})}(t^{(i^t_{new})}), t^{(i^t_{new})}]$ using Eq. (38) through (40) and consider the correlation constraint given in Eq. (41) during the identification.

      Check the quality of the surrogate model using Eqs. (31) through (35) and obtain $\varepsilon_r^{\max}$.

    End while

    Compute $p_f(t_0, t_e)$ using $\hat{g}(\mathbf{X}, \mathbf{Y}, t)$ and Eq. (36).

    Compute $Cov_{pf} = \sqrt{(1 - p_f(t_0, t_e)) / (p_f(t_0, t_e)) / N_{MCS}}$

    $q = q + 1$

End while

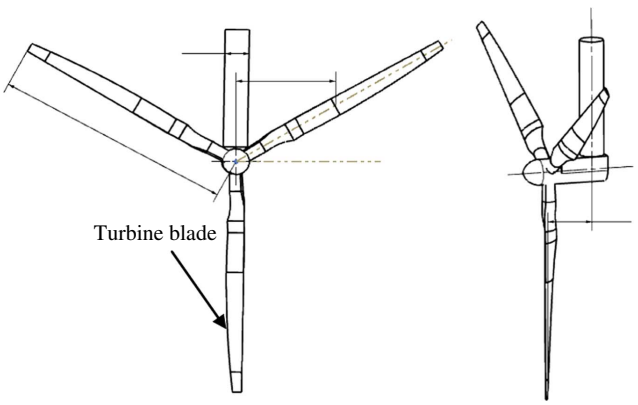

Fig. 2 Illustration of a hydrokinetic turbine

proposed reliability analysis method and load model, we did not consider the effect of rotation to simplify the problem.

The time-dependent failure probability of the turbine blade is given by

$$p_f(t_0, t_e) = \Pr\{G(\tau) = S_{\max}(\tau) - S_{\text{mat}} > 0, \quad \exists\, \tau \in [t_0, t_e]\} \tag{42}$$

where $S_{\max}$ is the maximum stress and S_{mat} is the strength of the material. $S_{\max}$ is a function of the river flow velocities acting on the turbine blade. In Sec. 5.2, we will discuss how to perform stress analysis for a given river flow velocity profile on the blade.

5.2 Stress Analysis. From the load analysis, it is found that the turbine blade is subjected to an edgewise moment generated

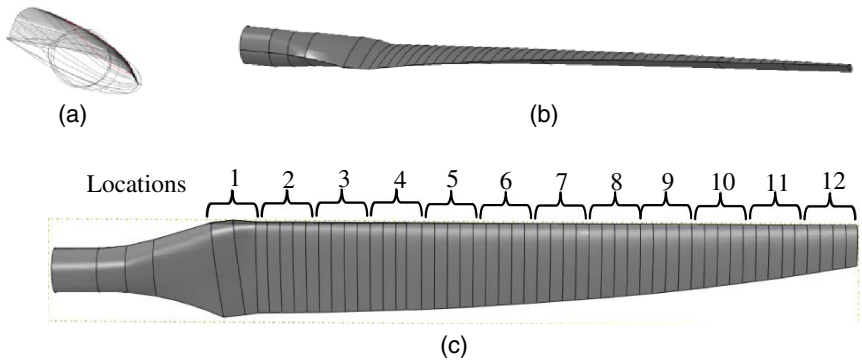

Fig. 3 Geometry configuration of the turbine blade: (*a*) side view locations, (*b*) front view, and (*c*) top view

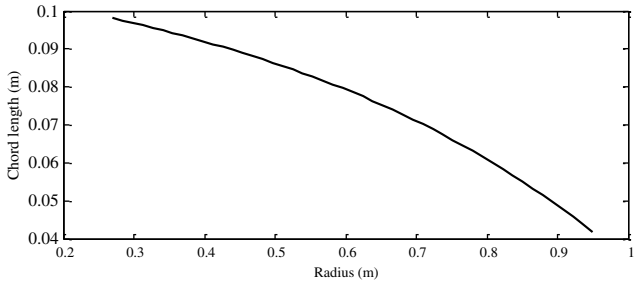

Fig. 4 Chord length distribution of the turbine blade

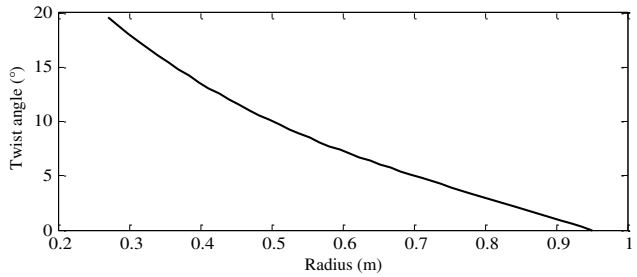

Fig. 5 Twist angle distribution of the turbine blade

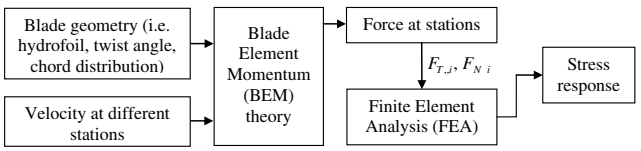

Fig. 6 Flowchart of the stress analysis for the turbine blade

from the edgewise force F_T and a flapwise moment generated from the flapwise force F_N. In order to compute F_T and F_N, the turbine blade is divided into 48 stations along the radial direction. The radius at station i is given by

$$r_i = r_{\text{root}} + i(1 - r_{\text{root}})/48 \tag{43}$$

where $r_{\text{root}} = 0.2$ meter is the root of the turbine blade.

After the discretization, the edgewise force $F_{T,i}$ and flapwise force $F_{N,i}$ at station i are computed using the blade element momentum (BEM) theory [57] based on the geometry of the turbine blade, local pitch, and the river velocity at the station. More details about the load analysis of the turbine blade are available in Ref. [57]. After the forces at stations of the turbine blade are obtained, they are input into finite element analysis (FEA) to get the stress response of the blade. Figure 6 gives the flowchart of the stress analysis. Figure 7 plots a snapshot of the stress analysis results of the turbine blade. In the stress analysis, nonlinearity is not considered. The maximum stress of the turbine blade is therefore independent from the strength of the material.

The stress response of the turbine blade is governed by the river flow velocity at different stations. In this paper, velocities at different stations are modeled using the Vine-ARMA model to account for the correlation and tail dependence over time and space. In addition, for the sake of illustration, it is assumed that the velocities at every four stations are the same. There are therefore totally 12 correlated stochastic processes (as indicated in Fig. 3(*c*)) that need to be modeled using the Vine-ARMA approach.

5.3 Simulation of River Velocity Using the Vine-ARMA Model. Assume that the Vine-ARMA model is trained based on experimental data. Since there are 12 stochastic processes, there are totally 66 copulas in the Vine structure (C-Vine is used in this example). Tables 3 and 4 give the families and parameters of the 66 bivariate copulas. All the marginal distributions of the 12 stochastic processes are assumed to be two-parameter Weibull distribution. Table 5 gives the parameters of the 12 Weibull distributions. For the 12 ARMA models of the associated Gaussian stochastic processes, the noise terms are assumed to be zero-mean Gaussian distributions with standard deviations as $[\sigma_{\varepsilon_i,(t)}, i = 1, 2, \ldots, 12] = [0.52, 0.45, 0.44, 0.27, 0.36, 0.33, 0.37, 0.57, 0.56, 0.32, 0.40, 0.56]$. Tables 6 and 7 present the AR and MA coefficients of the 12 ARMA models.

Based on the parameters of the Vine copula and ARMA models, the river flow velocities at locations 1 to 12 as indicated in Fig. 3(*c*) are simulated using the algorithm given in Table 1. Figure 8 gives one realization of the stochastic processes at four of the locations, and Fig. 9 depicts the velocity samples at several locations at a given time instant. It shows that the correlation over time and locations as well as the tail-dependence are maintained in the Vine-ARMA model as can be seen in Fig. 9.

5.4 Time-Dependent Reliability Analysis Using SILK-Vine-ARMA Model. We then perform time-dependent reliability analysis based on the simulated river velocities using the SILK method. In time-dependent reliability analysis, the Poisson ratio υ and the strength of the material S_{mat} are assumed to be random variables given by $\upsilon \sim \text{LN}(0.3, 0.02)$ and $S_{\text{mat}} \sim \text{LN}(210,50)$, where $\text{LN}(\mu, \sigma)$ is the lognormal distribution with mean μ and standard deviation σ. In order to verify the accuracy of the proposed method, a surrogate model is trained first for $S_{\max}$ using the FEA model given in Sec. 5.2 with a large number of training points (i.e., 900). The trained surrogate model $S_{\max}$ is then used to substitute the original model, as directly performing MCS on the original model is computationally prohibitive. Hereinafter, we call it the "high-fidelity surrogate model." We first compare the developed Vine-ARMA model and the multivariate ARMA model by performing MCS on the high-fidelity surrogate model. The multivariate ARMA model is trained based on the same sample as the Vine-ARMA model. Table 8 gives the results comparison between the Vine-ARMA model and multivariate ARMA (MARMA). It shows that the MARMA model overestimates the probability of failure which is consistent with what is expected because the Clayton copulas which have lower-tail dependences are used in the Vine-ARMA models (as shown in Table 3).

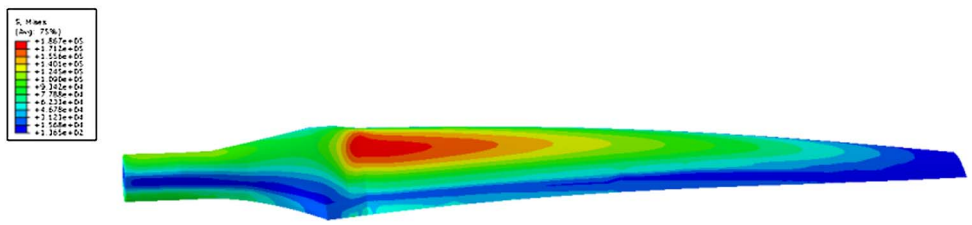

Fig. 7 von Mises stress response of the turbine blade

Table 3 Families of the bivariate copulas in the Vine copula

Copula no.	1	2	3	4	5	6	7	8	9	10	11	12	13	14	15	16	17
Family	2	2	2	3	3	3	3	2	2	2	3	3	2	2	3	3	3
Copula no.	18	19	20	21	22	23	24	25	26	27	28	29	30	31	32	33	34
Family	3	3	2	2	3	2	2	2	3	3	2	2	3	3	3	3	3
Copula no.	35	36	37	38	39	40	41	42	43	44	45	46	47	48	49	50	51
Family	2	2	3	2	2	2	3	3	2	2	3	3	3	3	3	2	2
Copula no.	52	53	54	55	56	57	58	59	60	61	62	63	64	65	66		
Family	3	2	2	2	3	3	2	2	3	3	3	3	1	1	1		

Note: Family "1" is "Gaussian," family "2" is "Student's t," and family "3" is "Clayton."

Table 4 Parameters of the bivariate copulas in the Vine copula

Copula no.	1	2	3	4	5	6	7	8
Parameter	(0.72, 3.5)	(0.65, 4.5)	(0.81, 3)	4.3	4.5	5.2	5.5	(0.87, 4.5)
Copula no.	9	10	11	12	13	14	15	16
Parameter	(0.61, 3)	(0.72, 6)	4.5	5.5	(0.83, 4)	(0.84, 2)	3.8	5.3
Copula no.	17	18	19	20	21	22	23	24
Parameter	3.2	4.5	5.2	(0.76, 5)	(0.65, 3)	4.5	(0.77, 3.5)	(0.61, 3)
Copula no.	25	26	27	28	29	30	31	32
Parameter	(0.72, 5.8)	3.7	4.1	(0.73, 5.2)	(0.93, 2)	5.2	4.8	3.7
Copula no.	33	34	35	36	37	38	39	40
Parameter	3.2	5.6	(0.66, 4.3)	(0.67, 2.5)	2.2	(0.67, 4.2)	(0.72, 3.5)	(0.71, 6.5)
Copula no.	41	42	43	44	45	46	47	48
Parameter	5.1	3.5	(0.83, 6)	(0.76, 3.5)	4.1	3.9	3.5	4.1
Copula no.	49	50	51	52	53	54	55	56
Parameter	5.2	(0.52, 5.2)	(0.74, 3.2)	4.1	(0.82, 5.1)	(0.59, 4.2)	(0.82, 7.1)	5.2
Copula no.	57	58	59	60	61	62	63	64
Parameter	4.5	(0.81, 5.5)	(0.81, 4.2)	3.4	3.2	4.2	3.4	0.68
Copula no.	65	66						
Parameter	0.72	0.89						

Table 5 Parameters of the 12 Weibull distributions

Distribution	1	2	3	4	5	6	7	8	9	10	11	12
Parameter 1	1.6	1.65	1.7	1.75	1.8	1.85	1.9	1.95	2.0	2.05	2.1	2.15
Parameter 2	2.7	2.72	2.74	2.76	2.78	2.80	2.82	2.84	2.86	2.88	2.90	2.92

Table 6 AR coefficients of 12 ARMA models

Location	1	2	3	4
AR coefficients	(0.72, −0.15, 0.21)	(0.82, −0.13, 0.10)	(0.79, 0.13, −0.12)	(0.88, 0.14, −0.09)
Location	5	6	7	8
AR coefficients	(0.77, −0.11, 0.25)	(0.77, −0.12, 0.24)	(0.82, 0.15, −0.10)	(0.72, −0.13, 0.11)
Location	9	10	11	12
AR coefficients	(0.72, −0.11, 0.15)	(0.88, 0.14, −0.21)	(0.77, −0.12, 0.24)	(0.72, −0.14, 0.18)

Note: $\varphi_j^{(0)} = 0$, the above coefficients are $\varphi_j^{(1)}, \ldots, \varphi_j^{(p)}$, $\forall j = 1, 2, \ldots, 12$.

Table 7 MA coefficients of the 12 ARMA models

Location	1	2	3	4	5	6
MA coefficients	(0.3, 0.12)	(0.35, 0.13)	(0.27, 0.12)	(0.23, 0.11)	(0.24, 0.15)	(0.52, 0.16)
Location	7	8	9	10	11	12
MA coefficients	(0.25, 0.11)	(0.3, 0.12)	(0.23, 0.10)	(0.52, 0.16)	(0.23, 0.11)	(0.22, 0.12)

We then perform time-dependent reliability analysis using the proposed Vine-ARMA-SILK method. Table 9 gives the results comparison of time-dependent reliability analysis obtained from the proposed method and MCS based on the high-fidelity surrogate model for the time duration of interest (0 to 150 mins). Note that we can compare the proposed method only with MCS, as MCS is the only currently available method for this kind of reliability analysis problem (as discussed in Sec. 4). The results show that the proposed method is able to perform time-dependent reliability analysis accurately and efficiently.

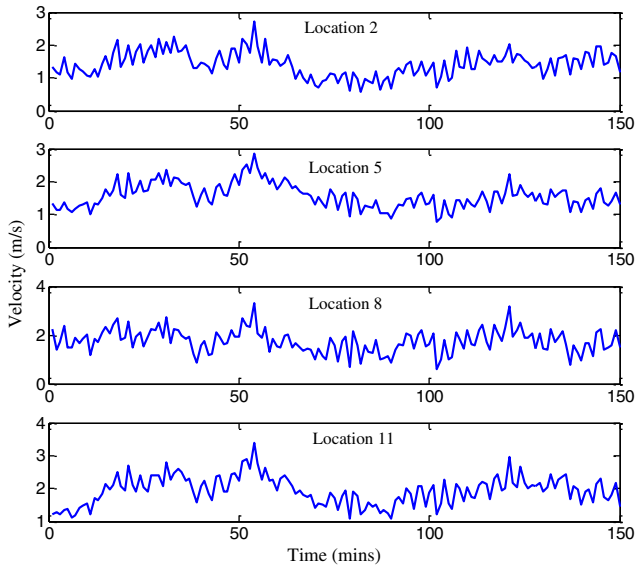

Fig. 8 One realization of simulated river velocities at four stations

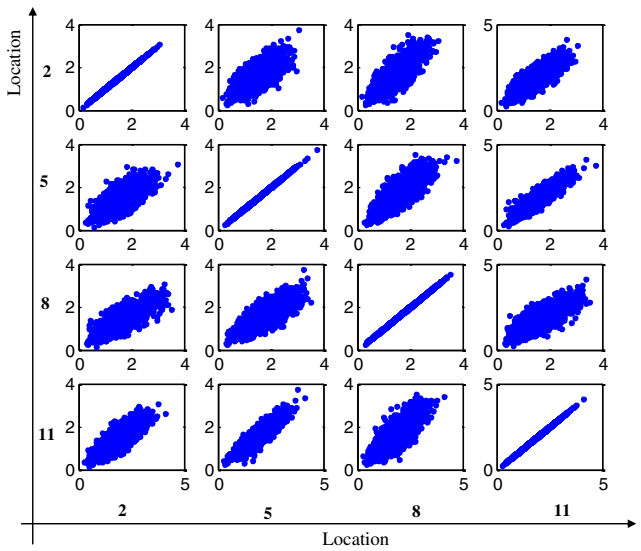

Fig. 9 Velocity at station *i* versus velocity at location *j*, $\forall i,j = 2,5,8,11$

Table 8 Results of turbine blade time-dependent reliability analysis

Method	$p_f(t_0, t_e)$	$\varepsilon(\%)$
MCS (Vine-ARMA)	0.0652	N/A
MCS (MARMA)	0.0712	9.10

NOF: number of function evaluations.

Table 9 Results of turbine blade time-dependent reliability analysis

Method	$p_f(t_0, t_e)$	NOF	$\varepsilon(\%)$
Proposed	0.0665	264	1.99
MCS (high-fidelity surrogate model)	0.0652	9.75×10^5	N/A

6 Conclusions

In practical applications, structures are often subjected to high-dimensional correlated and non-Gaussian stochastic load processes. Current methods for the modeling of such processes mainly rely on multivariate ARMA models. The multivariate ARMA model with Gaussian noise assumption has difficulty in capturing the tail dependence among different stochastic processes. In this paper, the Vine copula is combined with univariate ARMA models to model the correlated stochastic processes and accurately capture their tail dependence. In order to overcome the computational challenges in time-dependent reliability analysis caused by the introduction of Vine-ARMA model, the Vine-ARMA model is integrated with SILK surrogate modeling to efficiently and accurately estimate the time-dependent failure probability. A hydrokinetic turbine blade subjected to correlated river flow loads demonstrated the effectiveness of the proposed method.

Even though the Vine copula is able to flexibly model high-dimensional non-Gaussian copula and capture the tail dependence, the number of conditional distribution functions in the simulation of Vines will increase significantly with the dimension of the problem. For example, there are $(n-2)^2$ conditional distribution functions in the simulation of an n-variable D-Vine. Simulation of the Vine-ARMA model for a high-dimensional problem is computationally expensive. Improving the efficiency of the Vine-ARMA model simulation needs to be investigated in the future. In addition, the surrogate modeling-based method is used in this paper to substitute the computationally expensive simulation model. However, construction effort and accuracy of the surrogate model may suffer from the curse of dimensionality, as the number of variables and the nonlinearity in the problem increases. How to efficiently construct surrogate models for high-dimensional problems is an active research issue in the literature.

Acknowledgment

The research reported in this paper was supported by the Air Force Office of Scientific Research (Grant No. FA9550-15-1-0018, Technical Monitor: Dr. David Stargel). The support is gratefully acknowledged.

Appendix: Kriging Surrogate Model

The Kriging model of an unknown function $g(\mathbf{x})$ is given by [59]

$$\hat{g}(\mathbf{x}) = \mathbf{h}(\mathbf{x})^T \boldsymbol{\upsilon} + \varepsilon(\mathbf{x}) \tag{A1}$$

where $\boldsymbol{\upsilon} = [\upsilon_1, \upsilon_2, \ldots, \upsilon_p]^T$ is a vector of unknown coefficients; $\mathbf{h}(\mathbf{x}) = [h_1(\mathbf{x}), h_2(\mathbf{x}), \ldots, h_p(\mathbf{x})]^T$ is a vector of regression functions; $\mathbf{h}(\mathbf{x})^T\boldsymbol{\upsilon}$ is the trend of prediction; and $\varepsilon(\mathbf{x})$ is assumed to be a Gaussian process with zero mean and covariance $Cov[\varepsilon(\mathbf{x}_i), \varepsilon(\mathbf{x}_j)]$.

The covariance between two points $\mathbf{x}_i$ and $\mathbf{x}_j$ is given by

$$Cov[\varepsilon(\mathbf{x}_i), \varepsilon(\mathbf{x}_j)] = \sigma_\varepsilon^2 R(\mathbf{x}_i, \mathbf{x}_j) \tag{A2}$$

in which σ_ε^2 is the process variance and $R(\cdot,\cdot)$ is the correlation function.

For an untrained point $\mathbf{x}$, the expected value of the prediction is given by

$$\bar{g}(\mathbf{x}) = \mathbf{h}(\mathbf{x})^T\boldsymbol{\upsilon} + \mathbf{r}(\mathbf{x})^T\mathbf{R}^{-1}(\mathbf{g} - \mathbf{H}\boldsymbol{\upsilon}) \tag{A3}$$

where

$$\mathbf{r}(\mathbf{x}) = [R(\mathbf{x}, \mathbf{x}_1), R(\mathbf{x}, \mathbf{x}_2), \ldots, R(\mathbf{x}, \mathbf{x}_{n_s})] \tag{A4}$$

in which $\mathbf{x}_1, \ldots, \mathbf{x}_{n_s}$ are current training points.

The mean-square-error (MSE) of the prediction is given by [60]

$$\begin{aligned}\mathrm{MSE}(\mathbf{x}) = \sigma_\varepsilon^2\{1 - \mathbf{r}(\mathbf{x})^T\mathbf{R}^{-1}\mathbf{r}(\mathbf{x}) \\ + [\mathbf{H}^T\mathbf{R}^{-1}\mathbf{r}(\mathbf{x}) - \mathbf{h}(\mathbf{x})]^T(\mathbf{H}^T\mathbf{R}^{-1}\mathbf{H})^{-1} \\ \times [\mathbf{H}^T\mathbf{R}^{-1}\mathbf{r}(\mathbf{x}) - \mathbf{h}(\mathbf{x})] \qquad (A5)\end{aligned}$$

References

[1] Stewart, M. G., and Rosowsky, D. V., 1998, "Time-Dependent Reliability of Deteriorating Reinforced Concrete Bridge Decks," Struct. Saf., **20**(1), pp. 91–109.

[2] Kuschel, N., and Rackwitz, R., 2000, "Optimal Design Under Time-Variant Reliability Constraints," Struct. Saf., **22**(2), pp. 113–127.

[3] Mori, Y., and Ellingwood, B. R., 1993, "Reliability-Based Service-Life Assessment of Aging Concrete Structures," J. Struct. Eng., **119**(5), pp. 1600–1621.

[4] Hagen, Ø., and Tvedt, L., 1991, "Vector Process Out-Crossing as Parallel System Sensitivity Measure," J. Eng. Mech., **117**(10), pp. 2201–2220.

[5] Hagen, O., and Tvedt, L., 1992, "Parallel System Approach for Vector Out-Crossing," ASME J. Offshore Mech. Arct. Eng., **114**(2), pp. 122–128.

[6] Hu, Z., and Du, X., 2012, "Reliability Analysis for Hydrokinetic Turbine Blades," Renewable Energy, **48**(Dec.), pp. 251–262.

[7] Andrieu-Renaud, C., Sudret, B., and Lemaire, M., 2004, "The PHI2 Method: A Way to Compute Time-Variant Reliability," Reliab. Eng. Syst. Saf., **84**(1), pp. 75–86.

[8] Singh, A., and Mourelatos, Z. P., 2010, "On the Time-Dependent Reliability of Non-Monotonic, Non-Repairable Systems," SAE Int. J. Mater. Manuf., **3**(2010-01-0696), pp. 425–444.

[9] Singh, A., Mourelatos, Z., and Nikolaidis, E., 2011, "Time-Dependent Reliability of Random Dynamic Systems Using Time-Series Modeling and Importance Sampling," SAE Int. J. Mater. Manuf., **4**(1), 929–946.

[10] Wang, Z., Mourelatos, Z. P., Li, J., Baseski, I., and Singh, A., 2014, "Time-Dependent Reliability of Dynamic Systems Using Subset Simulation With Splitting Over a Series of Correlated Time Intervals," ASME J. Mech. Des., **136**(6), p. 061008.

[11] Mori, Y., and Ellingwood, B. R., 1993, "Time-Dependent System Reliability Analysis by Adaptive Importance Sampling," Struct. Saf., **12**(1), pp. 59–73.

[12] Wang, Z., and Wang, P., 2012, "A Nested Extreme Response Surface Approach for Time-Dependent Reliability-Based Design Optimization," ASME J. Mech. Des., **134**(12), p. 121007.

[13] Hu, Z., and Du, X., 2015, "Mixed Efficient Global Optimization for Time-Dependent Reliability Analysis," ASME J. Mech. Des., **137**(5), p. 051401.

[14] Sudret, B., and Der Kiureghian, A., 2000, "Stochastic Finite Element Methods and Reliability: A State-of-the-Art Report," Department of Civil and Environmental Engineering, University of California.

[15] Huang, S., Mahadevan, S., and Rebba, R., 2007, "Collocation-Based Stochastic Finite Element Analysis for Random Field Problems," Probab. Eng. Mech., **22**(2), pp. 194–205.

[16] Zhang, J., and Ellingwood, B., 1994, "Orthogonal Series Expansions of Random Fields in Reliability Analysis," J. Eng. Mech., **120**(12), pp. 2660–2677.

[17] Hu, Z., Mahadevan, S., and Du, X., 2015, "Uncertainty Quantification in Time-Dependent Reliability Analysis," ASME 2015 International Design Engineering Technical Conferences and Computers and Information in Engineering Conference, Aug. 2–7, American Society of Mechanical Engineers, Boston, MA, pp. V02BT03A062–V02BT03A062.

[18] Hu, Z., Mahadevan, S., and Du, X., 2016, "Uncertainty Quantification of Time-Dependent Reliability Analysis in the Presence of Parametric Uncertainty," ASCE-ASME J. Risk Uncertainty Eng. Syst., Part B: Mech. Eng., **2**(3), p. 031005.

[19] Ling, Y., Shantz, C., Mahadevan, S., and Sankararaman, S., 2011, "Stochastic Prediction of Fatigue Loading Using Real-Time Monitoring Data," Int. J. Fatigue, **33**(7), pp. 868–879.

[20] Ling, Y., and Mahadevan, S., 2012, "Integration of Structural Health Monitoring and Fatigue Damage Prognosis," Mech. Syst. Signal Process., **28**(Apr.), pp. 89–104.

[21] Wang, P., and Billinton, R., 2001, "Reliability Benefit Analysis of Adding WTG to a Distribution System," IEEE Trans. Energy Convers., **16**(2), pp. 134–139.

[22] Gupta, S., Shabakhty, N., and van Gelder, P., 2006, "Fatigue Damage in Randomly Vibrating Jack-up Platforms Under Non-Gaussian Loads," Appl. Ocean Res., **28**(6), pp. 407–419.

[23] Yang, L., and Gurley, K. R., 2015, "Efficient Stationary Multivariate NonGaussian Simulation Based on a Hermite PDF Model," Probab. Eng. Mech., **42**(Oct.), pp. 31–41.

[24] Li, W., and McLeod, A., 1981, "Distribution of the Residual Autocorrelations in Multivariate ARMA Time Series Models," J. Royal Stat. Soc. Ser. B, **43**(2), pp. 231–239.

[25] Boudjellaba, H., Dufour, J.-M., and Roy, R., 1994, "Simplified Conditions for Noncausality Between Vectors in Multivariate ARMA Models," J. Econometrics, **63**(1), pp. 271–287.

[26] Garel, B., and Hallin, M., 1995, "Local Asymptotic Normality of Multivariate ARMA Processes with a Linear Trend," Ann. Inst. Stat. Math., **47**(3), pp. 551–579.

[27] Jiang, C., Zhang, W., Han, X., Ni, B., and Song, L., 2015, "A Vine-Copula-Based Reliability Analysis Method for Structures With Multidimensional Correlation," ASME J. Mech. Des., **137**(6), p. 061405.

[28] Bedford, T., and Cooke, R. M., 2002, "Vines: A New Graphical Model for Dependent Random Variables," Ann. Stat., **30**(4), pp. 1031–1068.

[29] Joe, H., 1994, "Multivariate Extreme-Value Distributions With Applications to Environmental Data," Can. J. Stat., **22**(1), pp. 47–64.

[30] Cooke, R. M., "Markov and Entropy Properties of Tree-and Vine-Dependent Variables," Proceedings of the ASA Section of Bayesian Statistical Science.

[31] Cooke, R. M., and Goossens, L. H., 2004, "Expert Judgement Elicitation for Risk Assessments of Critical Infrastructures," J. Risk Res., **7**(6), pp. 643–656.

[32] Hu, Z., and Mahadevan, S., 2016, "A Single-Loop Kriging Surrogate Modeling for Time-Dependent Reliability Analysis," ASME J. Mech. Des., **138**(6), 061406.

[33] Hu, Z., and Du, X., 2015, "First Order Reliability Method for Time-Variant Problems Using Series Expansions," Struct. Multidiscip. Optim., **51**(1), pp. 1–21.

[34] Shumway, R. H., and Stoffer, D. S., 2009, *Time Series Analysis and Its Applications*, Springer, New York.

[35] Cochrane, J. H., 2005, "Time Series for Macroeconomics and Finance," Manuscript, University of Chicago.

[36] Joe, H., 1997, *Multivariate Models and Multivariate Dependence Concepts*, CRC Press, London.

[37] Sklar, M., 1959, "Fonctions de répartition à n dimensions et leurs marges," Université Paris 8.

[38] Deng, S.-J., and Jiang, W., 2005, "Levy Process-Driven Mean-Reverting Electricity Price Model: The Marginal Distribution Analysis," Decis. Support Syst., **40**(3), pp. 483–494.

[39] Kirchler, M., and Huber, J., 2007, "Fat Tails and Volatility Clustering in Experimental Asset Markets," J. Econ. Dyn. Control, **31**(6), pp. 1844–1874.

[40] Ditlevsen, O., Olesen, R., and Mohr, G., 1986, "Solution of a Class of Load Combination Problems by Directional Simulation," Struct. Saf., **4**(2), pp. 95–109.

[41] Ditlevsen, O., and Madsen, H. O., 1996, *Structural Reliability Methods*, Wiley, New York.

[42] Madsen, H. O., 1985, "Extreme-Value Statistics for Nonlinear Stress Combination," J. Eng. Mech., **111**(9), pp. 1121–1129.

[43] Aas, K., Czado, C., Frigessi, A., and Bakken, H., 2009, "Pair-Copula Constructions of Multiple Dependence," Insurance: Math. Econ., **44**(2), pp. 182–198.

[44] Bedford, T., and Cooke, R. M., 2001, "Probability Density Decomposition for Conditionally Dependent Random Variables Modeled by Vines," Ann. Math. Artif. Intell., **32**(1–4), pp. 245–268.

[45] Dissmann, J., Brechmann, E. C., Czado, C., and Kurowicka, D., 2013, "Selecting and Estimating Regular Vine Copulae and Application to Financial Returns," Comput. Stat. Data Anal., **59**, pp. 52–69.

[46] Joe, H., 1996, *Families of m-Variate Distributions With Given Margins and m (m-1)/2 Bivariate Dependence Parameters*, Lecture Notes-Monograph Series, Institute of Mathematical Statistics, Hayward, CA, vol. **28**, pp. 120–141.

[47] Kurowicka, D., and Cooke, R. M., 2006, *Uncertainty Analysis With High Dimensional Dependence Modelling*, Wiley, Chichester.

[48] Singh, N., 1994, "Forecasting Time-Dependent Failure Rates of Systems Operating in Series and/or in Parallel," Microelectron. Reliab., **34**(3), pp. 391–403.

[49] Czado, C., Brechmann, E. C., and Gruber, L., 2013, "Selection of Vine Copulas," *Copulae in Mathematical and Quantitative Finance*, Springer, Berlin/Heidelberg, pp. 17–37.

[50] Rosenblatt, M., 1952, "Remarks on a Multivariate Transformation," Ann. Math. Stat., **23**, pp. 470–472.

[51] Noh, Y., Choi, K., and Du, L., 2009, "Reliability-Based Design Optimization of Problems With Correlated Input Variables Using a Gaussian Copula," Struct. Multidiscip. Optim., **38**(1), pp. 1–16.

[52] Zhang, J., and Du, X., 2011, "Time-Dependent Reliability Analysis for Function Generator Mechanisms," ASME J. Mech. Des., **133**(3), p. 031005.

[53] Li, J., and Mourelatos, Z. P., 2009, "Time-Dependent Reliability Estimation for Dynamic Problems Using a Niching Genetic Algorithm," ASME J. Mech. Des., **131**(7), p. 071009.

[54] Echard, B., Gayton, N., and Lemaire, M., 2011, "AK-MCS: An Active Learning Reliability Method Combining Kriging and Monte Carlo Simulation," Struct. Saf., **33**(2), pp. 145–154.

[55] Hu, Z., and Mahadevan, S., 2016, "Global Sensitivity Analysis-Enhanced Surrogate (GSAS) Modeling for Reliability Analysis," Struct. Multidiscip. Optim., **53**(3), pp. 501–521.

[56] Hu, Z., Li, H., Du, X., and Chandrashekhara, K., 2013, "Simulation-Based Time-Dependent Reliability Analysis for Composite Hydrokinetic Turbine Blades," Struct. Multidiscip. Optim., **47**(5), pp. 765–781.

[57] Hu, Z., and Du, X., 2013, "Reliability Analysis for Hydrokinetic Turbine Blades Under Random River Velocity Field," Proceedings of the 7th Annual ISC Research Symposium, ISCRS 2013, April 23, Intelligent System Center, Missouri University of Science and Technology, Rolla, MO.

[58] Ramsay, R. R., Hoffmann, M., and Gregorek, G., 1999, "Effects of Grit Roughness and Pitch Oscillations on the S809 Airfoil: Airfoil Performance Report. Revised (12/99)," Technical Report NREL/TP-442-7817, Ohio State University, December, National Renewable Energy Laboratory (NREL).

[59] Rasmussen, C. E., 2006, *Gaussian Processes for Machine Learning*, MIT Press, Golden, CO.

[60] Lophaven, S. N., Nielsen, H. B., and Søndergaard, J., 2002, "DACE-A Matlab Kriging Toolbox, Version 2.0." Technical Report No. IMM-TR-2002-12, Technical University of Denmark.